1658

MAY 1980

PPPL-1658

UC-20f

DR. 1287

MASTER

VORTEX FORMATION DURING RF HEATING

BY

R. W. MOTLEY

PLASMA PHYSICS LABORATORY

PRINCETON UNIVERSITY
PRINCETON, NEW JERSEY

This work was supported by the U.S. Department of Energy Contract No. DE-AC02-76-CHO 3073. Reproduction, translation, publication, use and disposal, in whole or in part, by or for the United States government is permitted.

Vortex Formation During RF Heating of Plasma

R. W. Motley

Princeton University, Plasma Physics Laboratory
Princeton, New Jersey 08544

ABSTRACT

Experiments on a test plasma show that the linear theory of waveguide coupling to slow plasma waves begins to break down if the rf power flux exceeds ~30 W/cm^2. Probe measurements reveal that within 30 μs an undulation appears in the surface plasma near the mouth of the twin waveguide. This surface readjustment is part of a vortex, or off-center convective cell, driven by asymmetric rf heating of the plasma column.

I. Introduction

Radio frequency heating of fusion plasma to ignition has been a long term, still unrealized goal of many plasma scientists. One of several methods proposed to achieve this result is to irradiate a toroidal plasma with rf power from phased waveguide arrays.[1,2] This method is often referred to as lower hybrid heating,[3,4] since the excitation frequency is in the gigahertz range of frequencies, somewhat above the lower hybrid resonance frequency, $\omega_{LH} = \omega_{pi}/(1 + \omega_{pe}^2/\omega_{ce}^2)^{1/2}$ in the interior of the plasma. The engineering aspects of this type of heating are very attractive: high power megawatt vacuum tubes already exist; waveguide excitation minimizes the amount of coupling material, both metals and insulators, that must be placed near the hot reactor plasma.

The plasma physics aspects of lower hybrid heating, on the other hand, are not well understood. According to present plans, about 5 kW/cm^2 of power will be transmitted through phased waveguide arrays to the surface of toroidal plasmas. The evanescent guide fields, which extend a distance of $\sim k_z^{-1}$ from the mouth of the waveguide, excite electrostatic plasma waves to convey the power into the plasma core, where resonant absorption will transfer power to plasma electrons or ions. To ensure good coupling between electormagnetic and electrostatic waves, the mouth of the waveguide must be positioned

well within ~1 cm ($\sim k_z^{-1}$) of a moderate density plasma ($n > m_e\omega^2/4\pi e^2 \sim 10^{11} cm^{-3}$).

It is clear that nonlinear interactions will take place between the large amplitude plasma waves and the surface plasma. To date attention has been focussed on two types of interaction: (1) the parametric decay of lower hybrid waves into daughter waves[5] and (2) modification of the wave coupling by rf pressure effects.[6,7]

At the power levels needed to heat toroidal plasma the electron jitter velocity greatly exceeds the ion sound speed, so that the waves excited in the surface plasma are subject to parametric decay. If the interaction were strong, parametric cascading would lead to a serious power drain, since the short wavelength daughter waves would undergo resonant interaction with plasma particles well outside the plasma core. Fortunately, the decay process is convective, i.e., the ray vectors of the daughter waves do not align themselves parallel to the vectors of the parent waves, so that the strength of the interaction is limited.[5] The experimental evidence on waveguide excitation of lower hybrid waves, although limited, points to a weak interaction in the surface layers.[8-10]

Another nonlinear interaction becomes of importance if the rf pressure becomes comparable to the plasma pressure nkT—ponderomotive modification of the surface layers of the plasma. RF pressure effects have been observed in experiments using striplines[11] and rings[12-13] as wave exciters,

but have only recently been identified in waveguide excitation.[14]

Evidence for nonlinear effects on waveguide coupling has been obtained on the Petula,[15] Alcator A,[16] and JFT-2 Tokamaks.[17] We summarize the data as follows: At low power levels there is a strong variation of reflectivity with phase angle, as expected from the linear theory. Above a critical power level (0.1-1 kW/cm^2) the coupling becomes almost independent of phase angle. The reflectivity (at 180°) drops somewhat at moderate power levels, but at the highest power level obtained in Petula ~10 kW/cm^2, the reflectivity rises to ~30%. At present there is no explanation for these results.

In this paper we show that nonlinear waveguide coupling effects become measurable in a moderate density, low temperature test plasma above a power level of ~250 W, i.e., a power flux of ~25 W/cm^2 at the center of the waveguide. This power level is considerably above the threshold for parametric decay, but more than an order of magnitude less than that needed to demonstrate ponderomotive interactions. From detailed probe measurements near the mouth of the waveguide we conclude that the moderate increases in reflection observed result from the formation of an undulation in the plasma surface near the waveguide. The undulation itself is the first stage of readjustment of the plasma equilibrium, consisting

of a rotation about a center 0-1 cm from the mouth of the guide. A preliminary account of this work has already been published.[18]

The off-center plasma circulation studied here is a special case of vortex motion, which has previously identified and studied in experiments involving asymmetric plasma injection into magnetic traps[19] and plasma confinement in such devices as Q machines[20,21] and multipoles.[22,23] The plasma circulation is driven by electric fields at right angles to the magnetic field. Such fields can be generated in a plasma column by any disturbance to the equilibrium. An especially simple situation obtains if a plasma column terminated at the ends by conductors and confined by a strong magnetic field is heated asymmetrically. Thermal equilibration along the field lines occurs quickly, at the electron thermal speed. Equilibration across the field lines is hampered, however, by the slow cross-field thermal conductivity, so that large thermal gradients can be maintained for long periods in this direction.

The net current out of the plasma column, j, must be zero. If the end plates are non-emitting, the plasma assumes a positive potential V with respect to the end plates;[24]

$$j = j_i - j_e = nev_i - nev_e \exp(-eV/kT_e) = 0 \ , \qquad (1)$$

where v_i and v_e are the ion and electron velocities along the field lines. Since the ion flow velocity parallel to the

field is $v_i \cong v_e(m_e/m_i)^{1/2}$ (good if $T_i/T_e \ll 1$), then a cross-field temperature gradient ∇T_e will give rise to an electric field $E = -\nabla V$ of

$$\tilde{E} = -\frac{\nabla kT_e}{2e} \ell n\, m_i/m_e \,. \tag{2}$$

In response to this field the plasma (both electrons and ions) will drift at a velocity

$$\bar{v}_D = c\,\frac{\bar{E}\times\bar{B}}{B^2} \,, \tag{3}$$

provided the radius of curvature of the drift contours (the isothermal lines) is much greater than the ion cyclotron radius.[21] In a 6.5 kG field a thermal gradient of 1 eV/cm in an argon plasma will give rise to a drift velocity of $\sim 8.6 \times 10^4$ cm/sec. Such a velocity is readily detected if the heating pulse exceeds ~5 μs.

II. Survey of Linear Coupling Theory

The coupling between electromagnetic waves in a metallic guide and electron plasma waves is determined by the surface plasma within a distance $\sim k_\pi^{-1} < 1$ cm of the waveguide. External measurements of the reflection coefficient then provide valuable clues to the behavior of the surface plasma. To better understand the nonlinear modifications described in this paper, we outline in this section the predictions of linear theory.

Before describing the results of the boundary value problem, it is instructive to consider the reflection and transmission of plane electromagnetic waves incident on a plasma immersed in a strong magnetic field in the z-direction ($\omega_c/\omega >> 1$) and characterized by a linear density gradient, $\nabla n \approx n_c/\ell_c$, in the x-direction, where n_c is the cutoff density ($m_e \omega^2/4\pi e^2$) and ℓ_c is the separation between the waveguide and the cutoff layer.[25,26] Inside the plasma the wave solution representing an inward-travelling wave can be represented by the Airy Functions Ai and Bi

$$E_z = B\,(Ai(v) - iBi(v)), \tag{4}$$

where B is a constant, and $v = [(n_\perp - 1)\, k_o^2 \ell_c^2]^{1/3}(1-x/\ell_c)$. The amplitude of the applied guide field E_z^2 falls off over a distance δ near the cutoff layer, where

$$\delta(v=o) = \left[\frac{1}{E_z^2}\frac{\partial E_z^2}{\partial x}\right]^{-1} = 1.37\, k_o^{-1}[k_o\ell_c/(n_\perp^2-1)]^{1/3} . \tag{5}$$

For our conditions ($n_\perp \sim 3$, ℓ_c = 1-2 mm) δ = 5-6 mm.

To calculate the reflection coefficient of an incident electromagnetic wave, it is convenient to define a surface impedance Z[25] at the point x = 0 ,

$$Z = -\frac{E_z}{B_y} \tilde{=} 1.2\,(n_\perp^2 - 1)^{2/3}(k_o\ell_c)^{1/3}(1+i/\sqrt{3}) . \tag{6}$$

The fields of the plasma wave are then to be matched by the field of a TE_{10} mode in a waveguide. The waveguide impedance Z_w is real and depends only on the width of the guide, a ,

$$Z_w = (1-\lambda_o^2/4a^2)^{-1/2}.$$

The impedance units have been chosen such that Z(free space)=1. Once the impedance has been defined one can immediately draw on standard transmission line theory[27] to yield the reflection parameter

$$\rho = \frac{Z-Z_w}{Z+Z_w} \qquad (7)$$

and the reflection coefficient $\rho\rho^*$.

Reflection curves as a function of $n_\parallel$ are given in Fig. 1 for $Z_w = 1$ and $Z_w = 2$, a waveguide excited within 13% of cutoff. The effect of the finite waveguide is to shift the reflection curves to higher values of $n_\parallel$. High reflectivity occurs for low $n_\parallel$, where the plasma load approaches a short circuit, and at high $n_\parallel$, where the plasma is an open circuit. Optimal matching occurs for $n_\parallel^2 \sim 1 + 0.76\, Z_w^{3/2}/(k_o \ell_c)^{1/2}$, when the real part of the surface impedance matches the waveguide impedance. Perfect matching cannot be achieved without inductive tuning, because the surface impedance is complex. For our conditions ($Z_w \sim 1$, $\nabla n \sim 10^{12}\text{cm}^{-3}$, and $n_\parallel \sim 3$) the reflection coefficient should range between 7 and 15%.

For a complete solution to the boundary value problem, in which the higher order modes, as well as the dominant mode, are included, we turn to the theory of Brambilla.[2] The reflectivity of our twin, teflon-loaded waveguide as a

function of density gradient is displayed in Fig. 2. The different curves for both 180° and 0° excitation show how the reflection is affected by increasing separation between plasma and guide. For zero separation there is a ~10/1 variation in reflection between 0° and 180°-4% versus 40%. With the separation increasing to 3 mm the ratio decreases to ~2/1. Further separation would drop the ratio below 1 as the load changes from plasma to vacuum.

One can also calculate the power spectrum emitted by the twin guide, as shown in Fig. 3. This curve reveals an undesirable feature of the twin waveguide—there is a resonance near $n_{\parallel} \simeq 1$. This portion of the spectrum gives rise to waves within the plasma that do not satisfy the accessibility criterion, so that the waves remain trapped in the surface layers.

We illustrate the trapping phenomenon in Fig. 4, which is a mapping of the ray vectors from a point source. In the ray-tracing code, based on the eikonal approach,[28] the electromagnetic as well as the electrostatic terms in the dispersion relation have been included for our conditions (B = 6.5 kG, $n_e = 2 \times 10^{12}$). The critical $n_{\parallel}$ to ensure surface penetration is 1.9. By referring to Fig. 3 one can determine that ~60% of the power radiated by the twin guide remains trapped on the plasma surface. It is this component of the radiation that preferentially heats the surface layers of the plasma and triggers the nonlinear behavior discussed in section IV.

Evidence for the existence of a significant non-penetrating surface wave component of the wave field has been presented in the literature.[8,29]

III. The Experiment

The experiment was performed on the linear H-1 plasma source,[30] which produces a plasma column 2 m long and 10 cm in diameter, confined by a magnetic field of 6.5 kG in the measurements reported here. The plasma was created in a $\sim 3 \times 10^{-4}$ torr argon background by pulsing a ring electrode at one end of the column with ~5 kW of power at 155 MHz. The rf excitation yields an argon ion density of $1\text{-}2 \times 10^{12}$ cm^{-3} and an (initial) electron temperature of ~7 eV.

A twin teflon-loaded waveguide was positioned at the edge of the plasma column near the mid plane[29] (Fig. 5). Each element of the guide, 5.8 cm high and 1.9 cm wide, was excited in the TE_{01} mode, with the electric field aligned along the magnetic field. Five to 100 μsec bursts of power at up to 1 kW from a 2.45 GHz magnetron were sent into the phased waveguide during the afterglow of the main argon discharge. In our experiments the rf power density just outside the waveguide was $\leq$ 80 W/cm^2, so that the ratio of wave pressure to plasma pressure was $\leq 10^{-2}$. The plasma column was overdense, with n/n_c = 15-25. Both incident and reflected power were monitored by means of directional couplers and calibrated detectors.

An 8.6 mm microwave interferometer allowed us to infer the average electron density of the plasma column. Local density, electron temperature, and space potential were measured with two Langmuir probes. One could be translated axially and (primarily) horizontally on a 12 cm radial arc; the other was fixed axially, but could be moved across the column horizontally, and vertically along an arc. It is important to note that the circular trajectory of the latter probe causes it to intersect the plasma surface 1.5 cm below the midplane.

The microwave interferometer showed clearly that reionization of the background gas (argon) was not a major factor in these experiments. Typically, the line averaged density would rise by 10~15% during a 40 μs, 1 kW rf pulse. The ion saturation current was not directly a measure of the plasma density, since the rf power increased the electron temperature from 1 to ~3-4 eV and the ion collection is weakly dependent on the electron temperature. From comparisons between microwave and probe measurements of density we infer that the ion current (at -45 volts bias) is approximately proportional to $n_i T_e^{0.3}$ in the limited temperature range between 1 and 4 eV. The electron temperature was calculated from the slope of the current-voltage characteristic of the probe. The space potential V_s can be calculated from the measured electron temperature T and floating potential V_F through the relation

$$V_s = V_F + (kT_e/2e)\ln \alpha\, m_i/m_e \cong V_F + 5.2\ kT/e\ ,$$

which is valid for an argon plasma if the electron velocity distribution is Maxwellian. The factor $\alpha \approx 0.41$ is needed to correct for the current imbalance created by the strong magnetic field; electrons are collected only along the field lines. All probe measurements were performed 1-5 μs after turnoff of the rf excitation to avoid smearing of the space potential by the oscillating rf potentials.

All probes were of the dual purpose, triaxial type capable of measuring the rf wave fields, as well as the plasma density and potential.

IV. Results

1. Reflectivity

From both linear theory and experiment it is known that the reflection coefficient of a phased waveguide should be a sensitive function of the phase angle between adjacent waveguide elements. Results from low power (~100 W) excitation of the twin guide show the expected variation[2] of reflectivity with phase (Fig. 6), ranging from ~40% when the two elements are excited in phase to ~4% when elements are excited out of phase. This is in good agreement with linear theory. Qualitatively, one can understand this variation as follows: 0° phasing favors the excitation of long wavelength, strongly reflecting surface waves, while 180° phasing favors short wavelength, penetrating slow waves.

Under more prolonged high power pulsing (>200 W) the reflection coefficient begins to change with time. As shown in Fig. 7, at 180° phasing the reflectivity increases from ~5% to ~12% in a 30-40 μs interval after the start of a 1 kW microwave pulse. Under the same conditions the (0°) reflectivity drops from 40% to 30%. The net effect, after ~40 μs, is that the wave coupling is somewhat less sensitive to the phase angle between the two guides.

2. Density Profiles

Since the reflectivity depends principally on the plasma density within a distance δ of the waveguide mouth, we examined this region closely with Langmuir probes. First results from the horizontal probe are shown in Fig. 8. From this data it appears that the plasma surface facing the waveguide is pushed inward ~1 cm in 20 μs, i.e., there is an inward velocity of 5×10^4 cm/sec. This perturbation is not confined to the immediate vicinity of the waveguide. As shown in Fig., 9 the density depression appears initially near the mouth of the guide. Then it expands along the column at a speed of ~10^6 cm/sec, about four times the sound speed in the argon plasma. Thus the perturbation is nonlocal.

There is an apparent inconsistency between the reflectivity measurements, showing only a small (<10%) variation in reflectivity and the interpretation of the probe data. Since the total plasma motion is comparable with the evanescent distance δ the change in reflectivity would imply a plasma motion of only ~2 mm (Fig. 2), but the probe data imply a motion about 5 times as great. This inconsistency suggests that the surface perturbation was, perhaps, more involved than a simple plasma movement away from the guide.

The simplest explanation for the observed plasma motion is that it is driven by unbalanced forces perpendicular to the magnetic field. If this is correct, then the perturbation should change sign on reversal of the magnetic field. In fact, as illustrated in Fig. 10, the plasma within 1 cm of the guide rises, rather than falls, during rf pulsing with the magnetic field directed in the opposite direction. This measurement suggested the presence of induced electric fields of order 1V/cm with symmetry differing from the cylindrical plasma symmetry.

The most revealing evidence for the plasma motion was obtained with the vertical probe. Vertical profiles of plasma density (corrected for electron temperature) near the waveguide are shown in Fig. 11. The midplane of the plasma column (with the waveguide in place) is normally 1-2 cm below

the center of the waveguide. Following the application of 1 kW of RF power, the plasma surface in contact with the guide appears to move upward 2-3 cm in ~20 μs. The motion is in the $\hat{S} \times \bar{B}$ direction, where $\hat{S}$ is a unit vector in the direction of power flow within the waveguide. From this data we conclude either that the plasma moves vertically upward or that the inward plasma motion (Fig. 8) below the midplane line is balanced by an outward movement above the midplane.

With this information we now possess a simple explanation of the minor (~10%) change in waveguide reflectivity. The plasma as a whole is not pushed away from the guide; instead, the plasma in contact with the guide slips vertically from just below the geometrical centerline to a position ~2 cm above the centerline. Effectively, the surface plasma density (weighted by the power flux within the guide) is somewhat smaller and the wave coupling correspondingly smaller (at 180^{o}).

3. Vortex Motion

A more complete understanding of the readjustment of the plasma equilibrium can be obtained by mapping the temperature and space potential contours immediately (within 1-5 μs) after termination of the rf power pulse. The target plasma is moderately collisional ($n \sim 10^{12}$ cm^{-3}, $T_e \sim 1$ eV, $\lambda_{ei} \sim 3$ cm) so that the lower hybrid waves should raise the electron temperature to 3-4 eV, at which point ionization and

excitation losses dissipate most of the power absorbed by collisions. Probe measurements of the electron temperature 1 cm from the waveguide following 1 kW rf pulses of varying magnitude are shown in Fig. 12. The electron temperature rises to 3 eV in 20 μs. It is very likely that the heating results from collisional processes alone. One estimates that a few percent of the power in the plasma waves should be dissipated in the main body of the plasma column by electron-ion collisions and that the temperature should rise to 3 eV by this mechanism alone in 28 μs, only 8 μs longer than the measured heating time. In addition, since a large fraction of the power (~50%) remains trapped on the surface, this region of the plasma column should experience more intense heating.

A horizontal scan of the electron temperature and space potential in the midplane of the waveguide is shown in Fig. 13. After 20 μs, 1 kW of microwave power heats the plasma electrons from 1 eV to 3-4 eV. The temperature rise is indeed greatest near the waveguide (~4 eV), dropping off horizontally such that $|\partial T/\partial x| \sim 0.4$ eV/cm. Under the same conditions the space potential is ~25 volts near the waveguide and falls off with distance, so that $|\partial V/\partial x| \sim 1.7$ V/cm. The measured electric field is thus $\sim -4 \nabla kT_e/e$ rather than $-5.6\ \nabla kT_e/e$ as predicted by Eq. (3). This difference could result from axial temperature gradients, or small departures from a Maxwellian electron distribution, ion heating, or perhaps a systematic error in the potential measurement.

Vertical scanning at three separate locations in front of the guide (Fig. 14) reveals that the electron temperature and space potential are greatest just above the midplane of the guide, falling off towards the top and bottom of the waveguide such that $|\partial T/\partial y| \sim 1$ eV/cm and $|\partial V/\partial y| \sim 3$V/cm. In summary, there is a hot spot and an accompanying potential hill just outside the mouth of the waveguide, with evidence of skewing towards the top of the guide. In the absence of rf power no temperature or potential gradients are discernable in the data.

We have also measured temperatures and potentials in plasma cross sections displaced axially along the field lines. Following a 20 μs, 1 kW rf pulse the temperature and potential gradients 20 cm from the waveguide are about 1/2 those measured near the guide; 40 cm from the guide the gradients are unmeasurably small.

The evolution of the plasma surface distortion is now clear. Electrons just outside the waveguide are more strongly heated than those in the main body of plasma and move quickly along the field lines from the hottest regions. To avoid excessive electron losses, the plasma in these regions assumes a higher potential, thereby creating electric fields transverse to the magnetic field. Under the crossed electric and magnetic fields the plasma near the guide flows across the magnetic field along the equipotential contours at $3\text{-}5 \times 10^4$ cm/sec, i.e., at ~1/6 of the sound speed. The flow contours, illustrated in Fig. 15, are loops centered near the mouth of the guide. Plasma near the bottom moves away from the guide; plasma near the top pushes toward the guide. Thus, as a

function of time the nose of the plasma in contact with the guide appears to drift upward at ~10^5cm/sec. The time evolution of the initial perturbation ($t \lesssim 30$ μs) is indicated in Fig. 16.

The plasma flow lines above the midplane appear to lead into the teflon-loaded waveguide; in this way a thermosiphon is developed, in which plasma is pumped from the bottom to the top of the waveguide. Away from the midplane the equipotential loops are closed so that after 40-60 μs some plasma can make the complete circuit from the top to the bottom of the guide.

From Fig. 9 it is evident that the density perturbation appears to move along the field lines at ~ 4 × sound speed. This behavior is not a result of axial plasma flow; instead, it merely reflects an axial diminution in the radial E fields. Near the guide the plasma drifts horizontally at ~5×10^4cm/sec; 20 cm downstream the horizontal velocity is only 1/2 as great. Therefore the apparent axial velocity is $\Delta Z/(t_1 - t_2) \sim 10^6$cm/sec where $t_1 - t_2$ is the time for the plasma to drift ~1 cm. Thus the vortex is not a localized disturbance near the waveguide; it expands along the plasma column at a speed much greater than the plasma flow speed. In the initial transient state there is axial as well as cross-field shear in the flow rates, accompanied by pressure gradients along the field lines.

The rise in reflectivity saturates in 30-40 μsec (Fig. 7) and tends to drop thereafter. Probe measurements below the

midplane show that there is an accompanying rise in density after this time. Two factors appear to influence the saturation: the ionization rate and the rotation of high density plasma from the top to the bottom of the guide. This "recycling" should begin in about the time it takes for the plasma to rotate ~1/4 the circumference of the vortex, i.e., $t \approx \pi/2rv_D$, where $r \approx 1$ cm is the radius of the vortex. For $v_D = 5 \times 10^4$ cm/sec, $t \approx 30$ μsec, close to the experimental value.

For standard conditions we were not able to demonstrate unequivocally the role of rotation in determining the saturation level. Ionization ($\Delta n/n \sim 0.15$ after 40 μsec) and plasma flow into the guide are complicating factors. However, under more extreme conditions (8 kW power and 13 kG field) 23 cm from the waveguide the recycling phenomenon is clear, as shown in Fig. 17. Following the initial collapse of the surface plasma, after 35 μsec a high density tongue of plasma moves vertically down below the midplane, creating a density peak and valley. Measurements at different horizontal positions show (in this higher power test) that the vertical velocity is 1.5×10^5 cm/sec. After 100 μsec the tongue makes a complete circuit and reappears near the top of the guide (not shown in Fig. 16). Near the waveguide the profile distortions are strongly modified by the intrusion of the guide; the density peak becomes a plateau.

To summarize the experimental evidence: Preferential surface heating of the magnetoplasma gives rise to an off-center vortex rotation of the plasma. The radius of the vortex is comparable to the depth of the surface layers (~1 cm): The rotation speed (~0.5 × 10^5cm/sec at 1 kW) is determined by the magnetic field and the temperature anisotropy. Initially (in 10-20 μs) the surface deformation assumes the form of a vertical undulation. Later (after ~40 μs) high density layers of plasma drift down in front of and behind the waveguide, terminating the rise in reflectivity.

5. Effects of Vortex Motion on Wave Coupling and Propagation.

The primary reason for studying rf-induced vortices is to understand their effect on waveguide coupling and lower hybrid wave propagation. The most obvious change, the almost threefold increase in reflection coefficient (Fig. 7), results from the misalignment between rf power density and the region of maximum plasma density. This relationship is made clearer in Fig. 2 , which shows the twin waveguide reflectivity as predicted by linear theory. In the theory the plasma density is assumed to increase linearly away from the waveguide and not to vary in the y-direction.

No theory presently exists that takes account of the vertical asymmetry in the plasma profile. We have, nevertheless, attempted to estimate the effect of the undulation on

the reflectivity by assuming linear theory holds, by dividing up the vertical section of the waveguide into 6 zones and by weighing the reflection for each zone by the power density in that zone. From the data in Fig. 16, and the linear theory of Fig. 2, we estimate that the reflectivity should initially be 4% and thereafter rise to 9% at 30 μs. These estimates are close to the measured reflectivities of Fig. 7 (within 3%), indicating that a "patched up" linear theory may still be applicable at our power levels.

Two further changes in the waveguide coupling can be discerned in our data: skewing in the vertical temperature profiles (Fig. 14) as the most strongly heated zone moves vertically, and a vertical shift in the resonance cone. Evidence for this shift was obtained by vertical scanning of the rf field structure at a position 23 cm from the waveguide. The data, given in Fig. 18, show that the cone structure rises by ~1-1/2 cm during a 40 μs, 1 kW rf pulse. This displacement is similar to and in the same direction as the vertical shift of the surface plasma, and thereby reflects merely the vertical shift in the point of maximum coupling.

The shift in the rf field structure is displayed more directly in Fig. 19, which shows the horizontal variation of the 2.45 GHz signal (αE_z^2) near the waveguide. Both above and below the midplane the signal falls off over 5-7 mm, in good agreement with Eq. (5). As one extends the pulse, however, the initially symmetric field structure (at 10 μs)

becomes highly asymmetric; above the midplane the rf signal becomes almost twice as great as the signal below. The maximum intensity shifts upward by ~1.5 cm in step with the nose of the plasma in contact with the guide.

It is possible that under different conditions the surface undulation may give rise to more drastic modifications in the wave fields. As a result of the profile modification the plasma surface facing the waveguide tilts, so that the group velocity may also tilt vertically. If, in addition, the vertical k vector becomes comparable to $k_{\parallel}$, the spectral distribution function may be modified. We have measured the wavelengths in the resonance cone ($\lambda_{\parallel}$ ~ 5 cm) and have detected no shift in wavelength with rf power, up to the 1 kW level. Under higher power excitation with open waveguide configurations, however, the wave spectrum and the mode structure may be modified.

V. Discussion

In this paper we report the first experimental evidence on the response of surface plasma to moderate power excitation of lower hybrid waves by a waveguide grill. At the power levels attained in our experiment (<80 W/cm^2) the surface close to the waveguide undulates as a result of cross-field convection driven by off-center heating of the plasma column. This surface distortion reacts back on the wave fields, increasing the reflectivity, slightly skewing the electron heating, and raising the position of the

resonance cone. After ~40 μs the distortion ceases to grow because of ionization and the feedback of high density layers into the rarefield plasma.

An extensive literature has evolved concerning the effects of parametric instabilities and ponderomotive forces on lower hybrid wave excitation and propagation, so that it is necessary to examine their influence, if any, on this experiment. Parametric instabilities, indeed, have been detected and reported in earlier work on twin waveguide excitation of plasma.[8] The parametric decay interaction was found to be very weak under our conditions: the power in the decay waves was always less than 1% of the power in the pump wave; no pump depletion was observed, i.e., the wave energy measured with rf probes was always proportional to the rf power in the waveguide, up to the 2 kW level; there is no need to invoke parametric heating in our experiment; electron-ion collisions are sufficient to explain the temperature rise.

Ponderomotive forces are also weak in our experiment. The parameter $E^2/8\pi nkT$, which measures the ratio of rf to plasma pressure, is only ~0.01. The density rippling to be expected along the field lines, $\Delta n/n \simeq (e\tilde{E}/m_e\omega v_e)2/4 \approx 0.03$,[31] is small and unobservable ($v_e^2 = kT_e/m_e$). In addition to these quantitative estimates, there is a qualitative difference between the surface modification from ponderomotive forces and from thermal eddies. The rf pressure expels electrons (and then

ions) along the field lines away from regions where $\tilde{E}^2$ is large. Therefore, the density cavity produced by rf pressure should be symmetric vertically, in sharp contradiction to the observed behavior. Finally, the ponderomotive density perturbation should be a local phenomenon, i.e., the cavity should expand at the local sound speed. The perturbation studied here, on the other hand, is nonlocal.

Ponderomotive effects, however, should play an important role in experiments on toroidal plasmas, where the power flux is 100 × greater than in our experiment. It is also difficult to see how vortices are to be avoided in these experiments. Although the surface temperatures and magnetic fields may be an order of magnitude greater, these parameters are offset by the power density, which will be ~100 × as great. Vortices should form under these conditions in ~1 msec, which is only a small fraction of the heating time.

The effects of mild vortex motion need not be deleterious. For example, if the surface density is too high for optimum waveguide coupling (as it tends to be in high field, high density tokamaks) plasma pumping by convective eddies may reduce the plasma surface density and waveguide reflectivity. In fact, moderate power (~1 kW/cm^2) wave fields applied to the Alcator A, Petula, and JFT-2 Tokamaks have

resulted in improved coupling and reduced sensitivity to waveguide phasing. Another possibility is that the plasma circulation may give rise to an enhanced thermal conductivity in the surface layers, so that the overall surface temperature is reduced. Surface cooling accompanying rf heating of tokamak plasmas has been observed by Suckewer and Hawryluk,[32] but has not yet been explained. Surface cooling is desirable, since it appears to reduce the evolution of high Z impurities from the vacuum walls.

Unfavorable consequences may also result from vortex excitation. Surface undulations reduce the effective cross section for power transmission, so that other nonlinear interactions, such as parametric instabilities and ponderomotive density rippling may be more severe. In tokamak experiments, open rather than loaded waveguide arrays are planned. Should the plasma drift into the open waveguide, the mode structure of the lower hybrid waves may be altered.

The results of this work cannot be applied immediately to heating experiments on toroidal plasmas, principally because of the great difference in background gas pressure. The gas pressure near the vacuum vessel varies considerably around the torus, but should be of the order ~1% of the pressure in our experiment (2×10^{-4} torr). The role of ionization in limiting the growth of the undulation should be greatly reduced in the tokamak experiments, so that the ultimate surface distortion may be more severe. On the other hand, if there is significant outgassing from plasma bombardment

of the waveguide, the surface instability could evolve into an intense surface discharge that traps and wastes a large fraction of the wave power, which then becomes unavailable for heating the plasma core.

It is clear that one should try to minimize the excitation of convective plasma loops in rf heating experiments by minimizing surface wave excitation. To this end one can try a variety of strategies, including using multiple waveguides, either active or passive, and reducing the power levels in the end guides.

One should not expect vortex formation to be confined solely to plasmas heated by lower hybrid waves. They will tend to form whenever a magnetically-confined plasma is heated asymmetrically. Hydromagnetic wave excitation by half-turn coils as well as neutral beam heating of (overdense) plasma columns may also generate vortices, especially in linear plasma columns. In toroidal plasmas one expects that the convective cell will be confined to the plasma surface beyond the limiter, since the rotational transform should smooth temperature and potential inhomogeneities.

Acknowledgments

We acknowledge with pleasure stimulating discussions with W. M. Hooke, S. Bernabei, and E. J. Valeo, the ray tracing calculations by F. J. Paoloni, the engineering assistance of C. Murko, and technical help from J. Frangipani. This work was done under DoE Contract No. DE-AC02-76-CHO-3073.

REFERENCES

1. P. Lallia, in Proc. 2nd Topical Conference on RF Plasma Heating (Texas Tech. University, Lubbock, Texas, 1974) paper C3.

2. M. Brambilla, Nucl. Fusion 16, 47 (1976).

3. W. M. Hooke, Course on "Instabilities and Confinement in Toroidal Plasma", International School of Plasma Physics, Varenna, 1971 (Commission of the European Community, Luxembourg, 1974) p. 269.

4. C. F. Karney and A. Bers, Mass. Inst. of Technology Report QPR 113, 105 (1974).

5. M. Porkolab and R. P. H. Chang, Rev. Mod. Phys. 50, 745 (1978).

6. G. J. Morales, Phys. Fluids 20, 1164 (1977).

7. N. R. Pereira, A. Sen, and A. Bers, Phys. Fluids 21, 117 (1978).

8. S. Bernabei, M. A. Heald, W. M. Hooke, R. W. Motley, F. J. Paoloni, M. Brambilla, and W. D. Getty, Nucl. Fusion 17, 292 (1977).

9. M. Porkolab, S. Bernabei, W. M. Hooke, R. W. Motley, and T. Nagashima, Phys. Rev. Lett. 38, 230 (1977).

10. T. Imai, T. Nagashima, T. Yamamoto, K. Uehara, S. Konoshima, H. Takeuchi, H. Yoshida and N. Fugisawa, Phys. Rev. Lett. 43, 586 (1979).

11. R. J. LaHaye, private communication.

12. R. L. Stenzel and W. Gekelman, Phys. Fluids 20, 108 (1977).

13. J. R. Wilson and K. L. Wong, Phys. Rev. Lett. 43, 1392 (1979).

14. R. W. Motley, W. M. Hooke, and C. R. Gwinn, to be published.

15. Petula Group, Contributed Papers to 9th European Conf. on Controlled Fusion and Plasma Physics (Culham Laboratory, Abingdon, Oxon., England, 1979) p. 21.

16. J. J. Schuss,et al., Phys. Rev. Lett. 43, 274 (1979).

17. T. Nagashima and N. Fujisawa, in Heating in Toroidal Plasmas, Vol. 2, Ed. by T. Consoli (Pergamon Press, Oxford, 1979) p. 281.

18. R. W. Motley, W. M. Hooke, and G. Anania, Phys. Rev. Lett. 43, 1799 (1979).

19. W. H. Bostick, Phys. Rev. 104, 292 (1956); 106, 404 (1957).

20. J. A. Decker, P. J. Freyheit, W. D. McBee and L. T. Shepherd, Phys. Fluids 10, 2442 (1967).

21. D. Mosher and F. F. Chen, Phys. Fluids 13, 1328 (1970).

22. R. A. Dory, D. W. Kerst, D. M. Meade, W. E. Wilson, and C. N. Erikson, Phys. Fluids 9, 997 (1966).

23. W. L. Harries, Phys. Fluids 13, 1751 (1970).

24. I. Langmuir and L. Tonks, Phys. Rev. 34, 876 (1929).

25. V. E. Golant, Zhur. Tech. Fiz. 41, 2492 (1971); Sov. Phys. Tech. Phys. 16, 1980 (1972).

26. V. Krapchev and A. Bers, Nucl. Fusion 18, 519 (1978).

27. S. Ramo, J. R. Whinnery and T. van Duzer, Fields and Waves in Communication Electronics (John Wiley and Sons, Inc., New York, 1965) p. 28.

28. T. H. Stix, The Theory of Plasma Waves (McGraw-Hill, New York, 1962) p. 58.

29. R. W. Motley, S. Bernabei, W. M. Hooke, R. McWilliams, and L. Olson, Plasma Physics 21, 567 (1979).

30. R. W. Motley, S. Bernabei, W. M. Hooke, and D. L. Jassby, J. Appl. Phys. 46, 866 (1975).

31. K. Matsuda, Y. Matsuda, and G. E. Guest, General Atomic Co. Report GA-A15351, 1979, unpublished.

32. S. Suckewer and R. J. Hawryluk, Phys. Rev. Lett. 40, 1649 (1978).

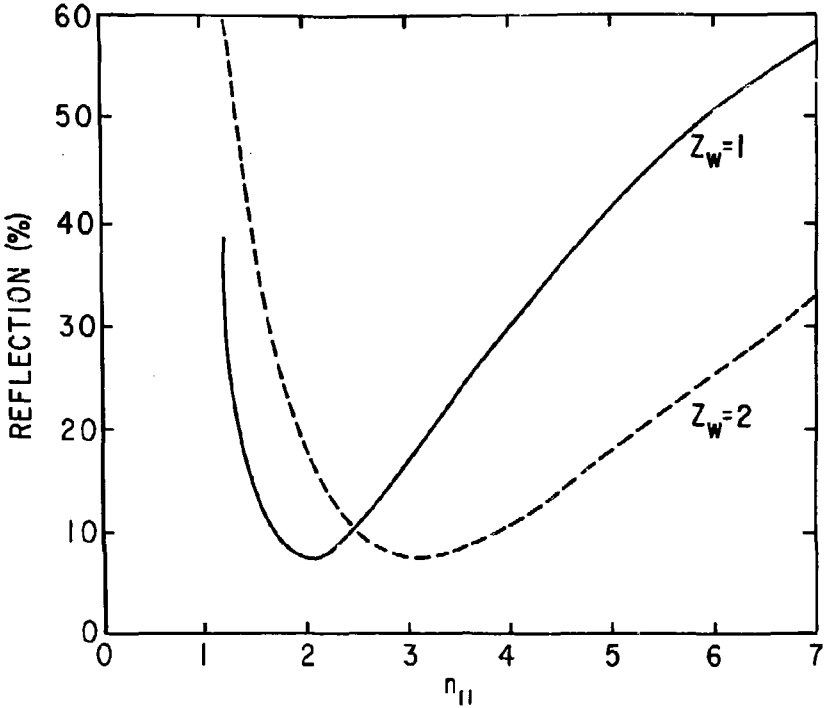

(PPPL-803448)

Fig. 1. Reflectivity $\rho\rho^*$ for plane waves incident on a plasma characterized by a density gradient of 10^{12} cm^{-4}. Calculations are shown for a waveguide with infinite extension in the y-direction ($Z = 1$) and for a guide excited within 13% of cutoff ($Z_w = 2$).

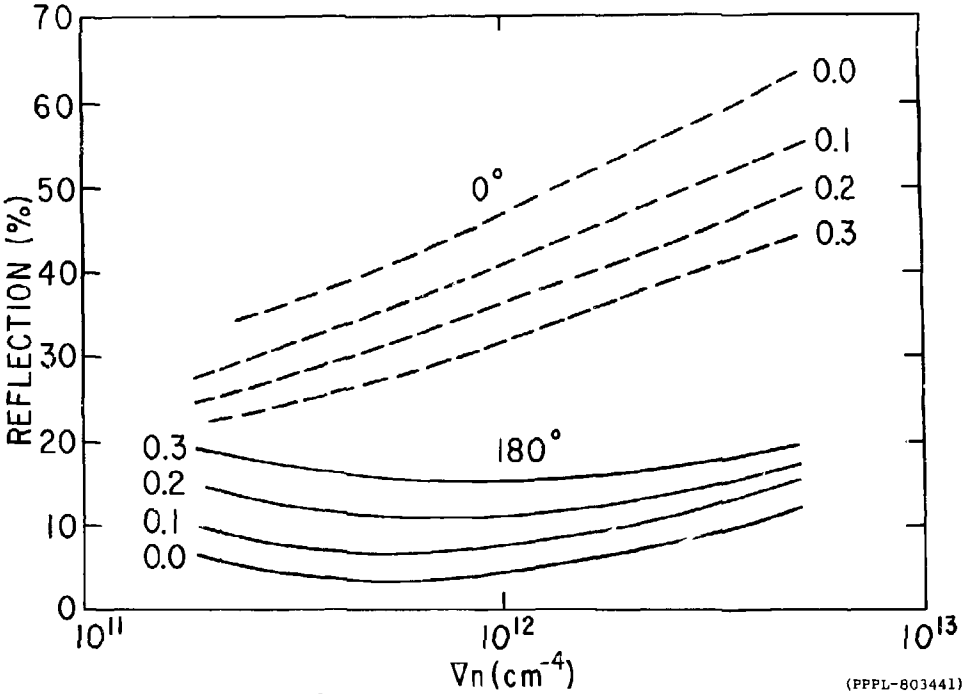

(PPPL-803441)

Fig. 2. Theoretical reflection[2] from a teflon-loaded twin waveguide, a = 1.9 cm, f = 2.45 GHz as a function of the density gradient. Solid lines show the reflection with 180° excitation; dashed lines, with 0° excitation. The parameters labelling each curve show the separation between plasma and waveguide.

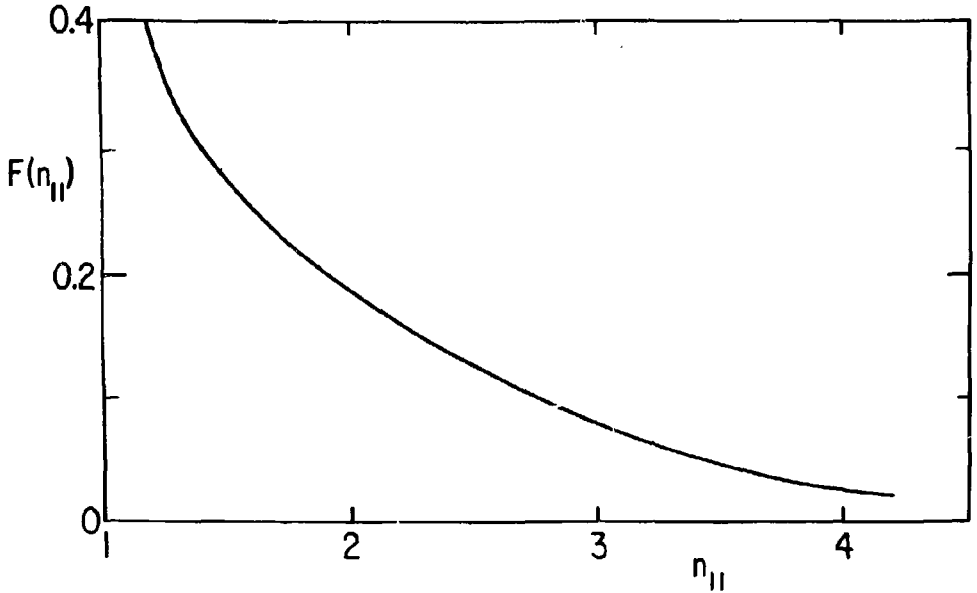

(PPPL-803442)

Fig. 3. (Parallel) wavenumber spectrum radiated by a twin waveguide; f = 2.45 GHz; a = 1.9 cm; $V_n = 10^{12}$ cm^{-4}.

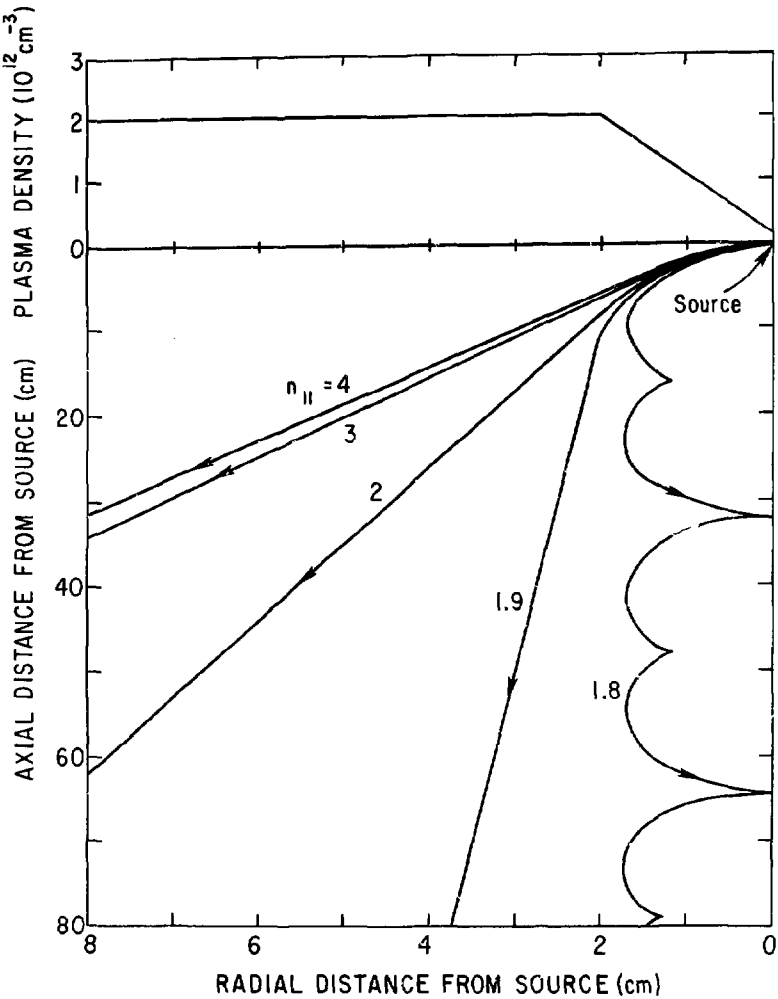

(PPPL-803445)

Fig. 4. Ray vectors radiated from a point source into a density ramp and plateau; f = 2.45 GHz, B ≈ 6.5 kG.

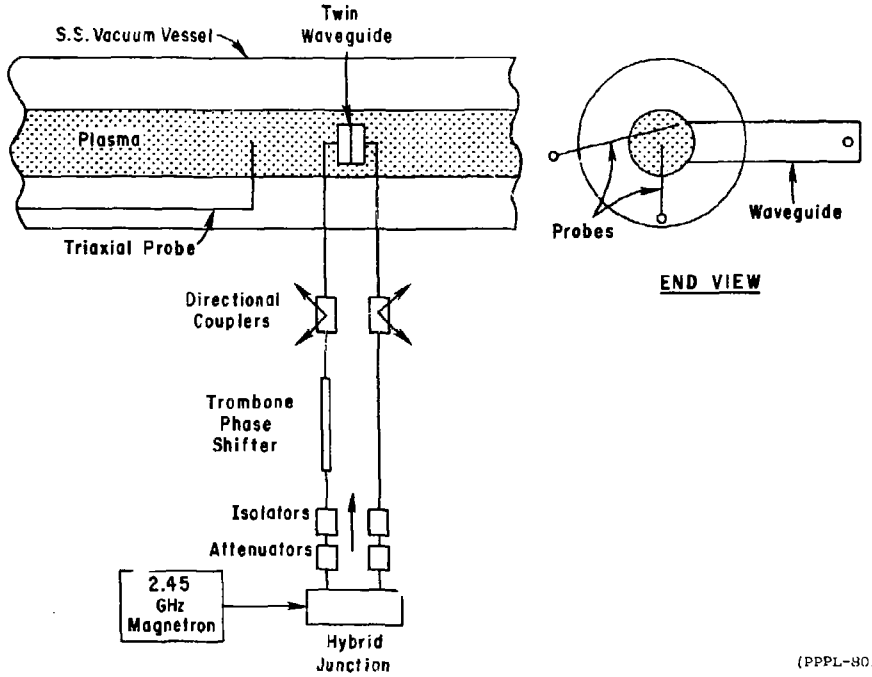

(PPPL-803444)

Fig. 5. Side and end view of plasma column, waveguide excitor, and triaxial probes. The side probe can be moved horizontally and vertically. The bottom probe can be moved axially and horizontally, in an arc.

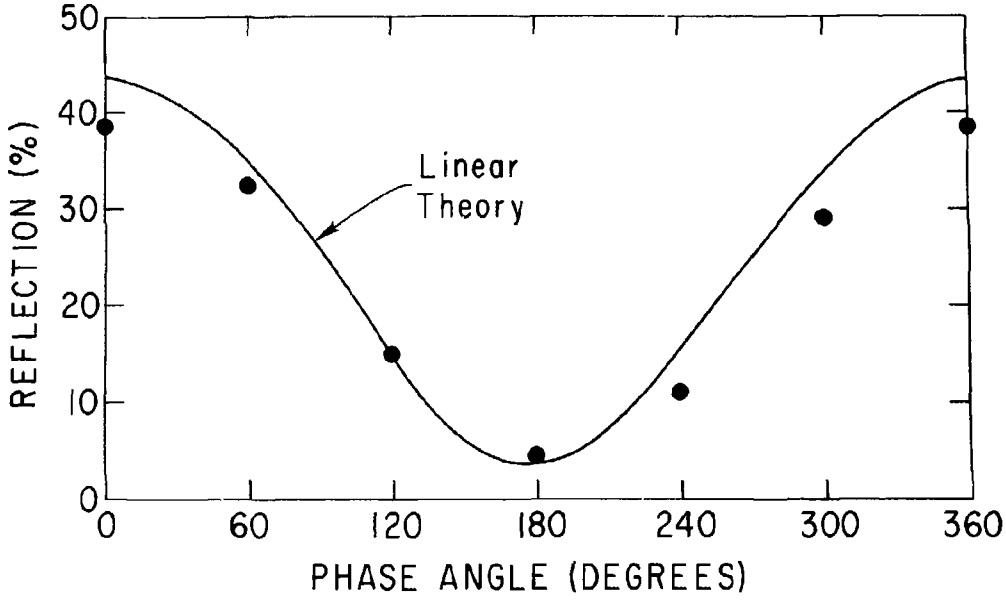

(PPPL-796056)

Fig. 6. Reflection from a twin waveguide as a function of the phase angle between the two elements. The power level was 100 watts, the plasma density 10^{12} cm^{-3}; $Vn \simeq 10^{12}$ cm^{-4}; B = 6.5 kG.

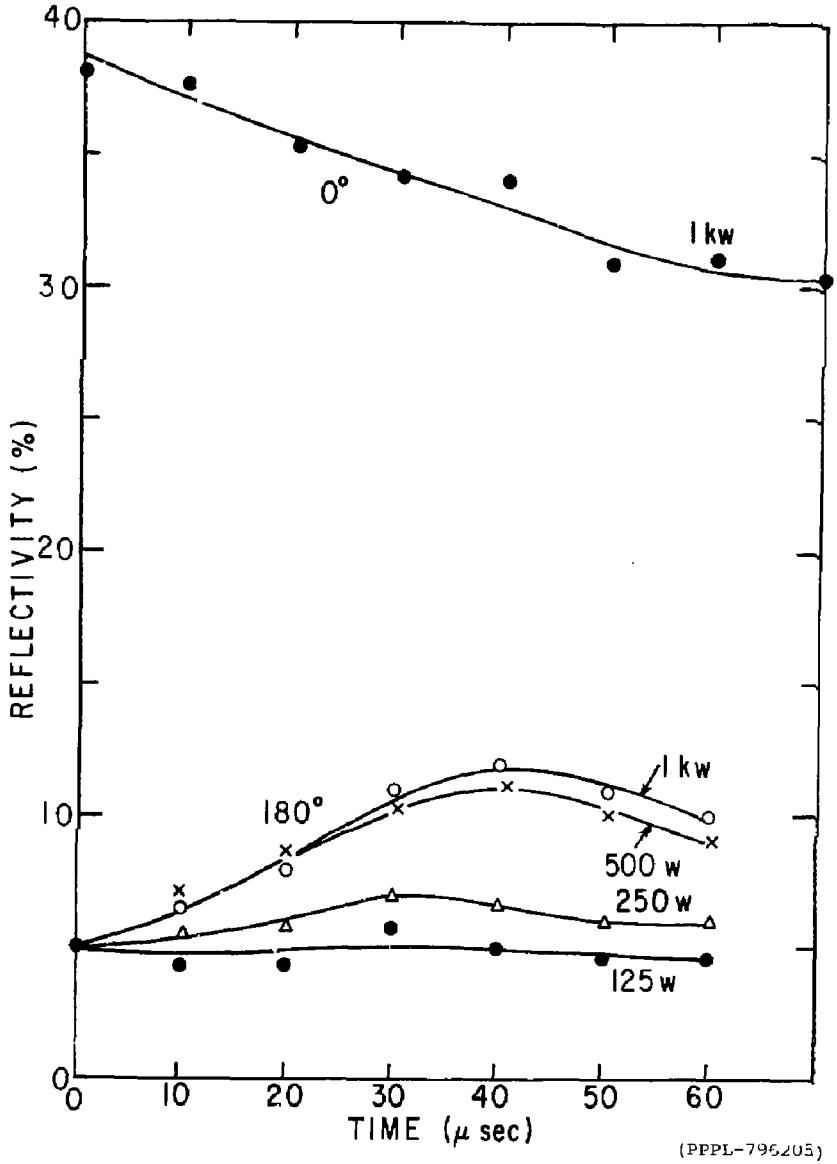

Fig. 7. Time development of the reflection coefficient for the twin guide with 0° and 180° phase difference between waveguide elements. The plasma density was ~10^{12} cm^{-3}, B = 6.5 kG.

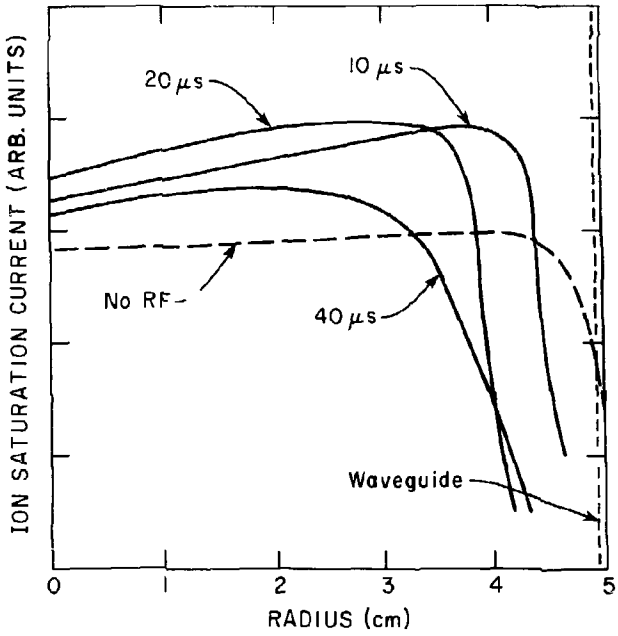

(PPPL-796060)

Fig. 8. Radial variation of ion current from the horizontal probe. Measurements were performed in a 0.5 μs interval following termination of a 1 kW microwave pulse. Near the guide the probe was 1.5 cm below the midplane.

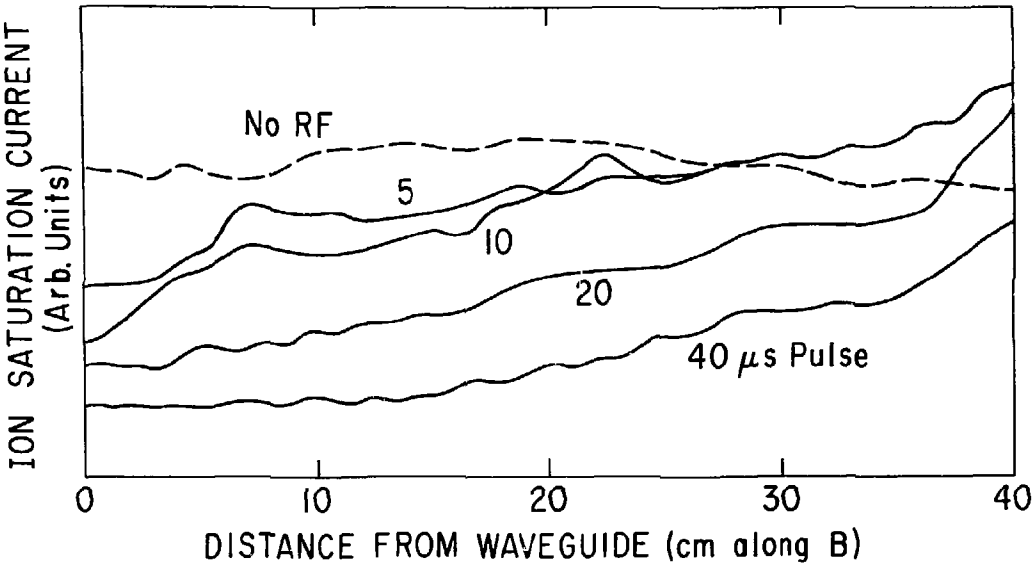

(PPPL-793696)

Fig. 9. Axial variation of the ion saturation current after 1 kW microwave pulses of varying duration. The probe was positioned 0.5 cm from the plasma edge, 1.5 cm below the midplane of the waveguide.

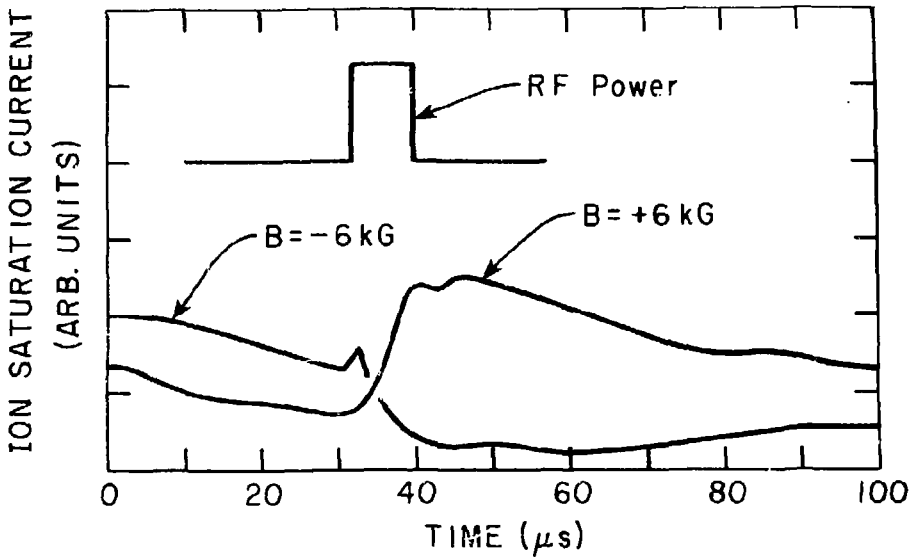

(PPPL-796057)

Fig. 10. Effect of reversing the axial magnetic field. Probe was positioned near the waveguide, 0.5 cm from the plasma edge and 1.5 cm below midplane.

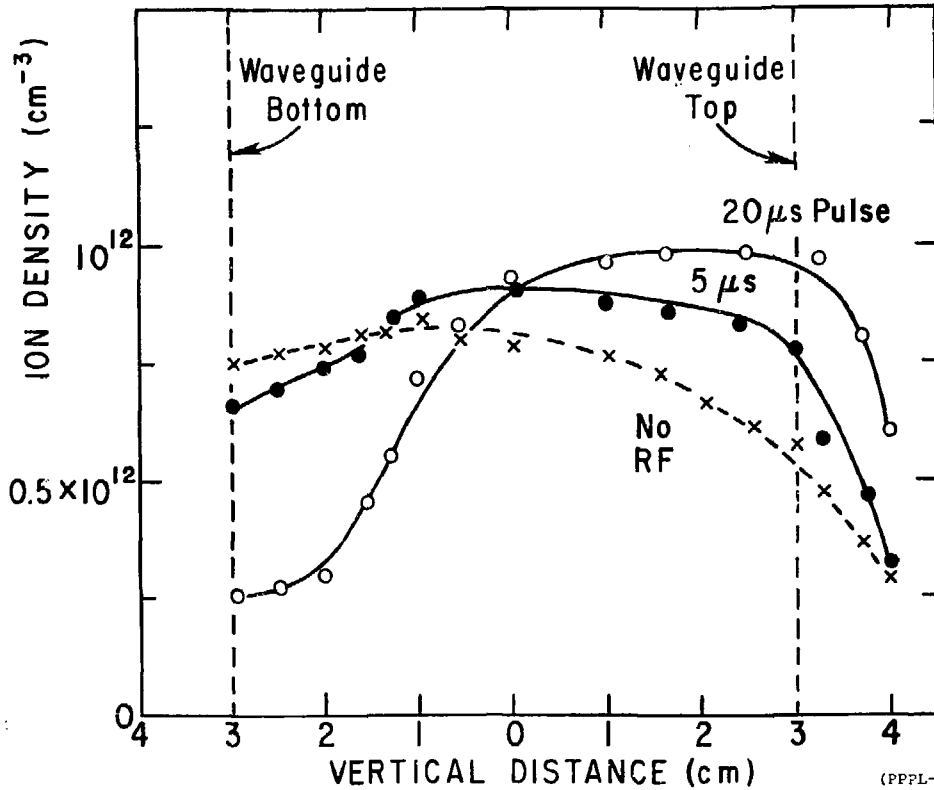

(PPPL-796207)

Fig. 11. Vertical scan of ion density (calculated from the ion saturation current) following 1 kW rf pulses of varying duration. The probe was positioned ~1 cm from the waveguide; B = 6.5 kG.

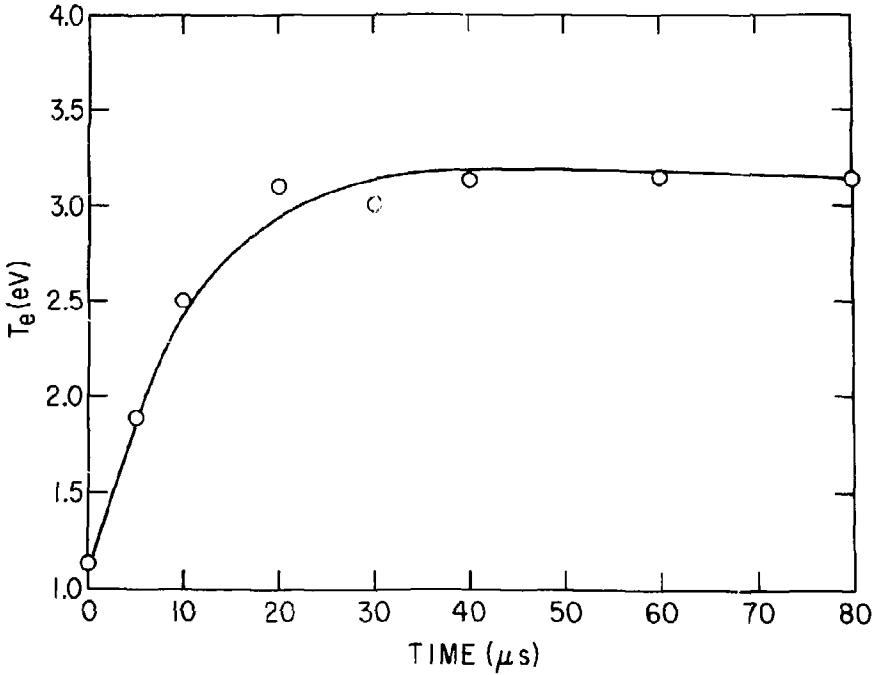

(PPPL-796058)

Fig. 12. Time variation of electron temperature following 1 kW microwave pulses of varying duration. The probe was located 1 cm from the guide.

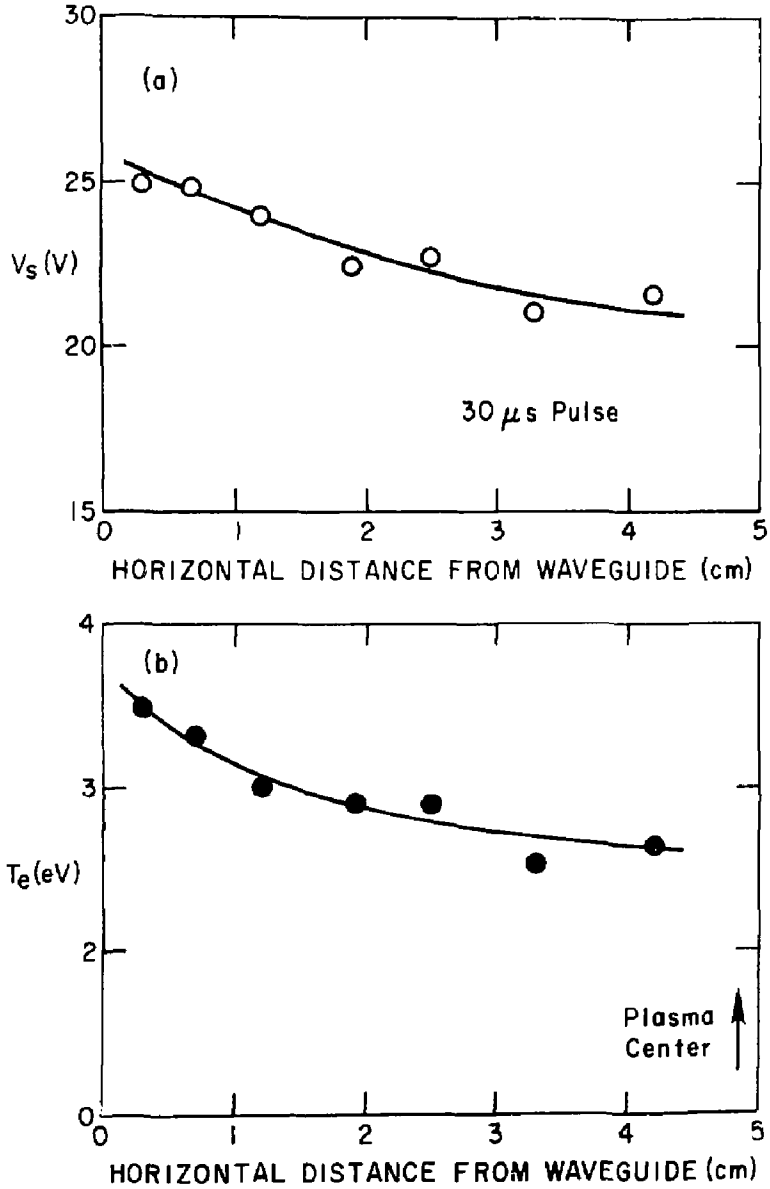

(PPPL-793697)

Fig. 13. Horizontal variation of electron temperature and space potential in a cross section near waveguide following a 20 μs, 1 kW rf pulse.

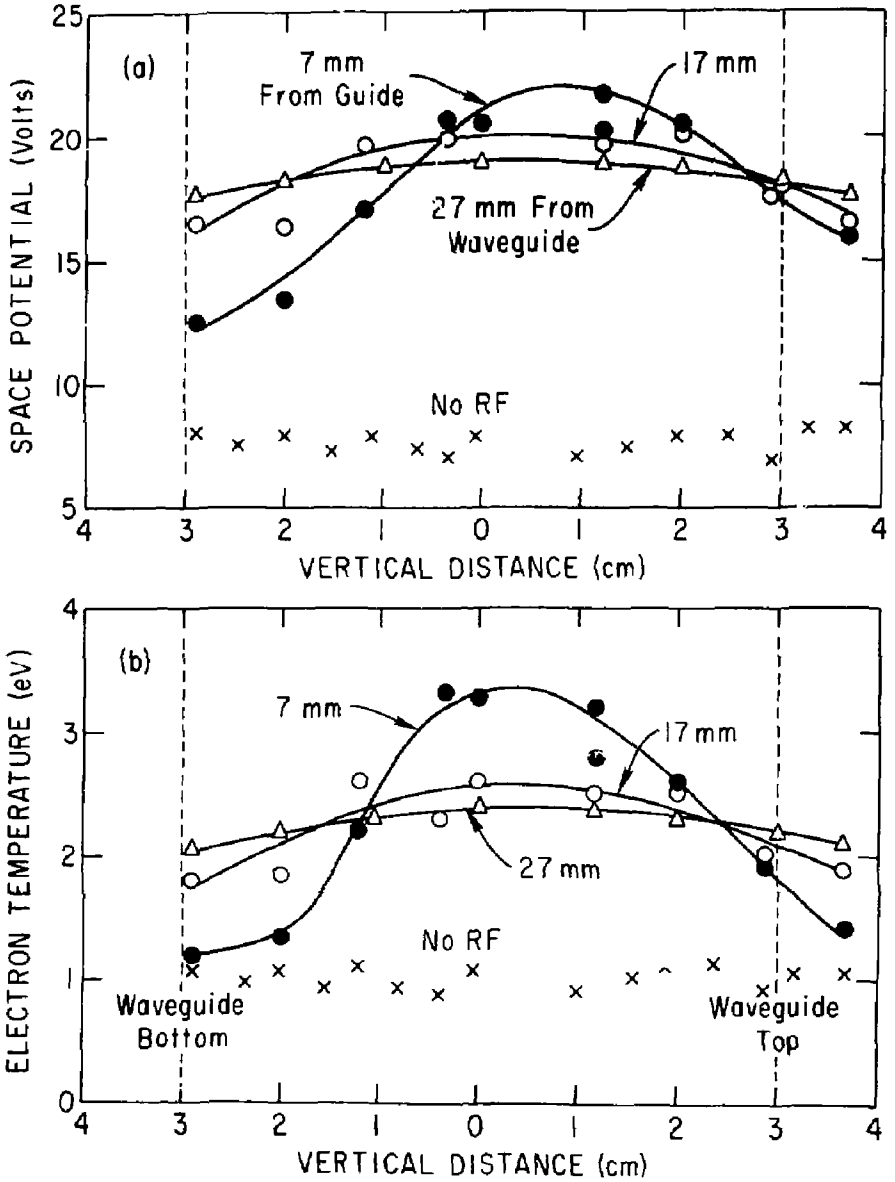

(PPPL-796059)

Fig. 14. Vertical scans of electron temperature and space potential following 20 μsec, 1 kW microwave pulses.

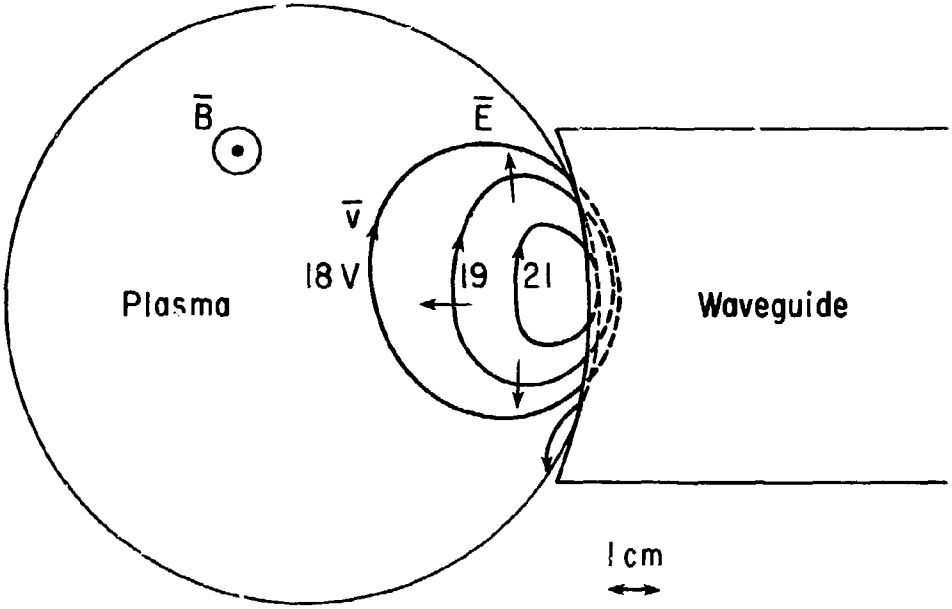

(PPPL-803446)

Fig. 15. Plasma flow patterns established by asymmetrical electron heating. Arrows show local direction of electric field. Numbers indicate space potential in volts.

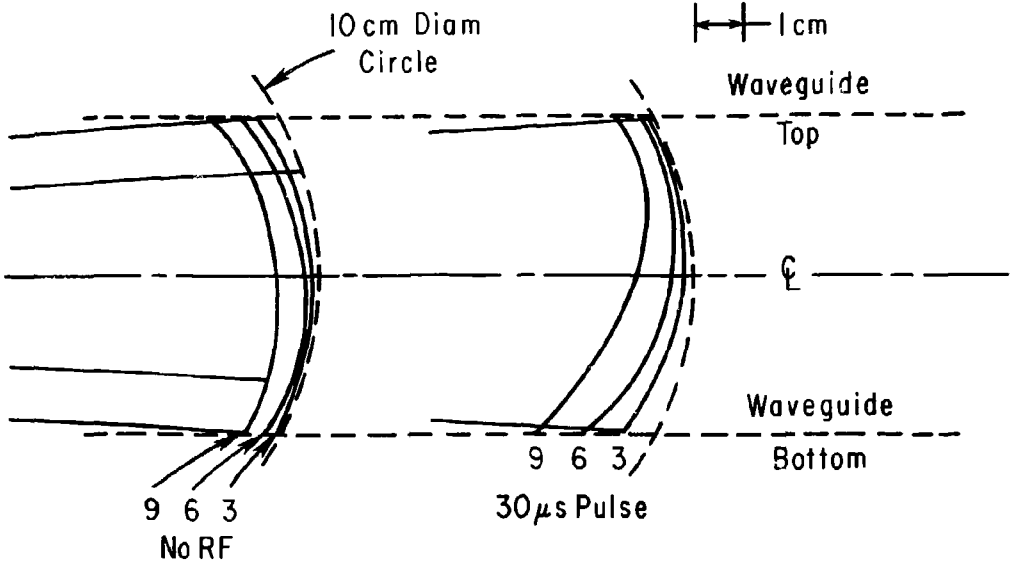

(PPPL-803440)

Fig. 16. Density contour patterns near the guide before and after a 30 μs, 1 kW rf pulse.

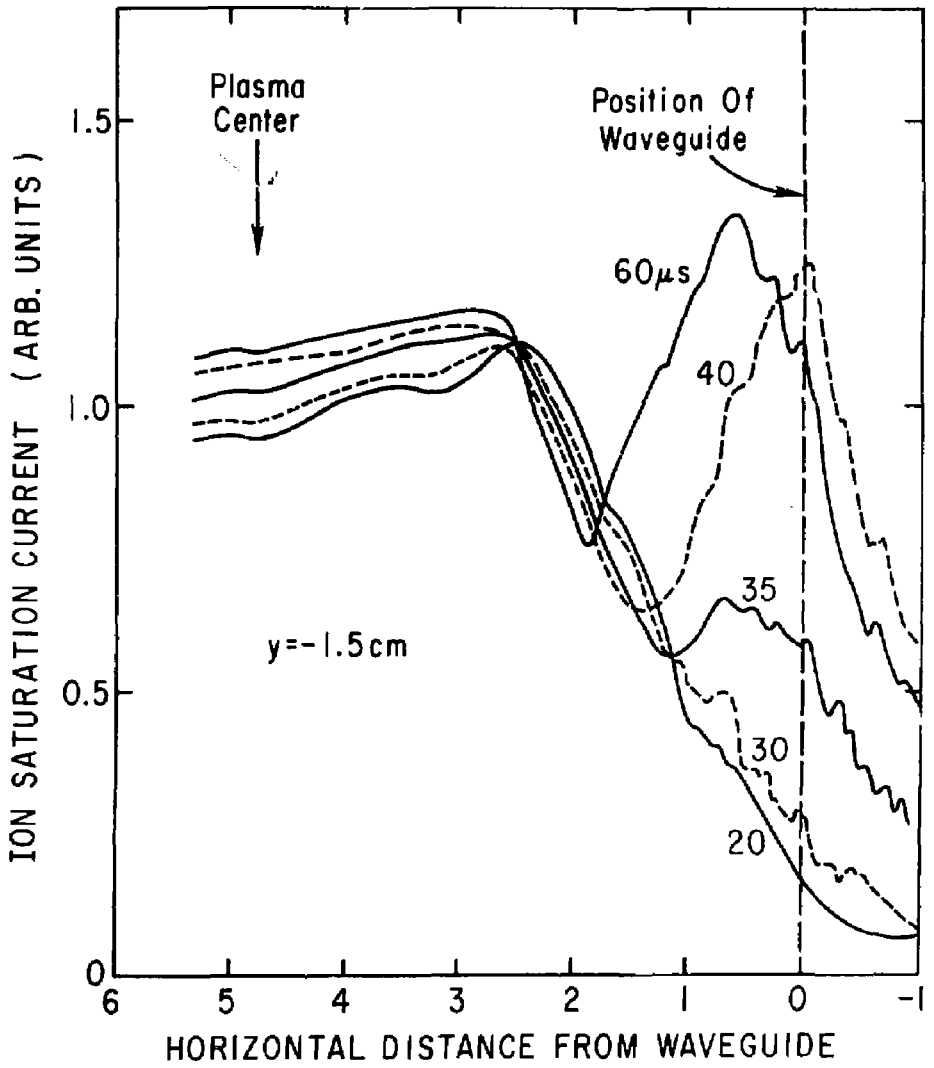

(PPPL-803447)

Fig. 17. Evolution of radial plasma profiles 23 cm from the waveguide under the following conditions: 8 kW rf power and 13 kG magnetic field.

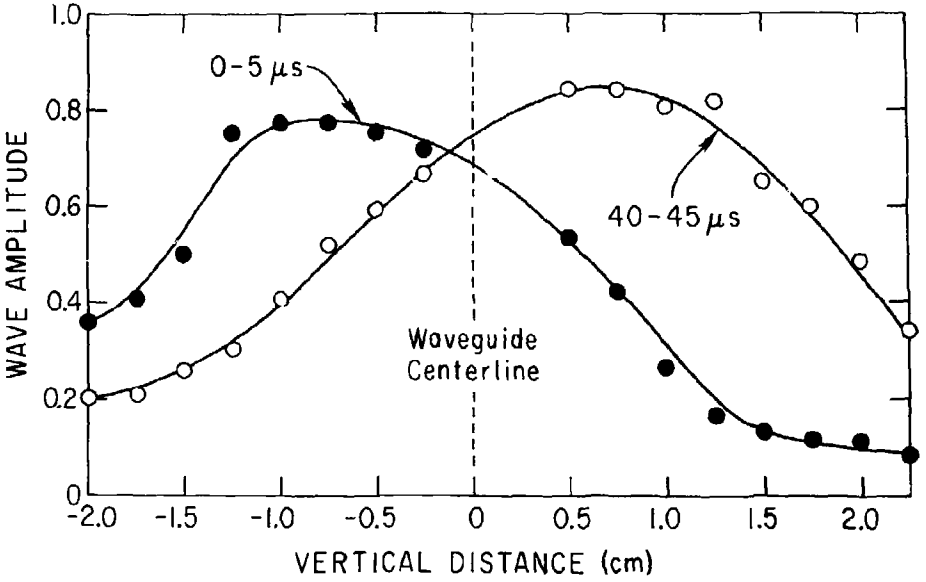

(PPPL-796053)
Fig. 18. Vertical rise of rf resonance cone measured 23 cm from the waveguide.

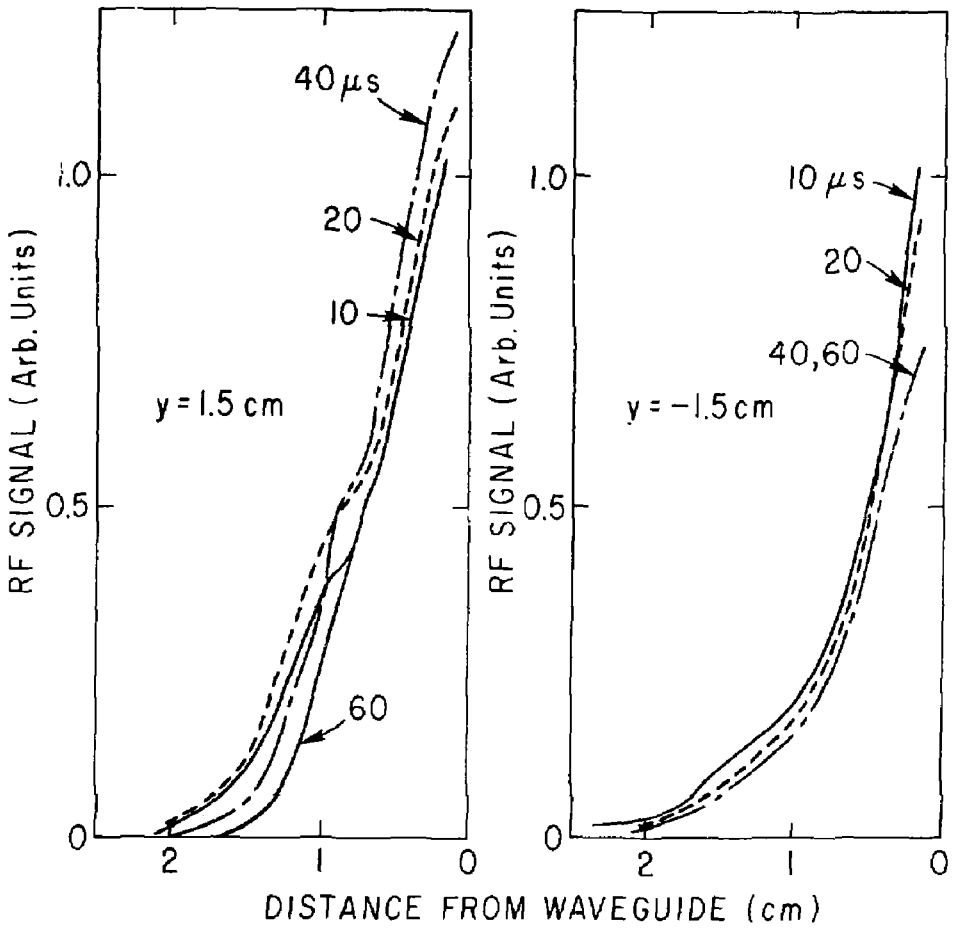

(PPPL-803577)

Fig. 19. Variation of the rf signal on a double-shielded "T" probe 10, 20, 40, and 60 μs after turning on a 1 kW lower hybrid pulse. Data are shown for horizontal scans 1.5 cm above and below the midplane.